Published OnlineFirst November 2, 2010; DOI:10.1158/0008-5472.CAN-10-1454

Cancer Research

Quantitative *In vivo* Imaging of the Effects of Inhibiting Integrin Signaling via Src and FAK on Cancer Cell Movement: Effects on E-cadherin Dynamics

Marta Canel, Alan Serrels, Derek Miller, et al.

Cancer Res 2010;70:9413-9422. Published OnlineFirst November 2, 2010.

Published OnlineFirst November 2, 2010; DOI:10.1158/0008-5472.CAN-10-1454

Cancer Research

Quantitative *In vivo* Imaging of the Effects of Inhibiting Integrin Signaling via Src and FAK on Cancer Cell Movement: Effects on E-cadherin Dynamics

Marta Canel[1], Alan Serrels[1], Derek Miller[2], Paul Timpson[2], Bryan Serrels[1], Margaret C. Frame[1], and Valerie G. Brunton[1]

Abstract

Most cancer-related deaths are due to the development of metastatic disease, and several new molecularly targeted agents in clinical development have the potential to prevent disease progression. However, it remains difficult to assess the efficacy of antimetastatic agents in the clinical setting, and an increased understanding of how such agents work at different stages of the metastatic cascade is important in guiding their clinical use. We used optical window chambers combined with photobleaching, photoactivation, and photoswitching to quantitatively measure (*a*) tumor cell movement and proliferation by tracking small groups of cells in the context of the whole tumor, and (*b*) E-cadherin molecular dynamics *in vivo* following perturbation of integrin signaling by inhibiting focal adhesion kinase (FAK) and Src. We show that inhibition of Src and FAK suppresses E-cadherin–dependent collective cell movement in a complex three-dimensional tumor environment, and modulates cell-cell adhesion strength and endocytosis *in vitro*. This shows a novel role for integrin signaling in the regulation of E-cadherin internalization, which is linked to regulation of collective cancer cell movement. This work highlights the power of fluorescent, direct, *in vivo* imaging approaches in the preclinical evaluation of chemotherapeutic agents, and shows that inhibition of the Src/FAK signaling axis may provide a strategy to prevent tumor cell spread by deregulating E-cadherin–mediated cell-cell adhesions. *Cancer Res; 70(22); 9413–22. ©2010 AACR.*

Introduction

In their physiologic environment, cells are in contact with surrounding extracellular matrix (ECM) and with neighboring cells. Although cell-matrix adhesions are largely integrin-based, cell-cell junctions are mediated by adherens junctions (AJ), tight junctions, and desmosomes. Cadherin-based AJs provide the initial means of cell-cell contact and have key roles during the development and maintenance of epithelial polarity (1, 2). Additionally, there is overwhelming evidence that E-cadherin is an important tumor and/or invasion suppressor (3–5). Tumor cells employ a number of strategies to move *in vivo*, either as individual cells or collectively as cohesive groups of cells that maintain cell-cell contacts (6). However, many tumors can adapt their mode of movement in response to external stimuli, and several lines of evidence support the idea of cross-talk between integrin-mediated cell-ECM interactions and E-cadherin–mediated cell-cell junctions that may be key to the plasticity observed in tumor cells (7, 8). Although the mechanisms involved are not understood, integrin-dependent modulation of Rho GTPases and the actomyosin cytoskeleton that is tethered at both adhesion types may play an important role (9). In addition, Src and focal adhesion kinase (FAK), two non–receptor tyrosine kinases that are key regulators of integrin-dependent matrix adhesions, have been linked to the control of AJs. Upon integrin engagement both FAK and Src tyrosine kinases are autophosphorylated on specific tyrosine residues at integrin-mediated adhesions. FAK autophosphorylation on Y397 creates a high-affinity binding site for the SH2 domain of Src, which leads to the Src-dependent phosphorylation of FAK on additional tyrosine residues. These act as protein-protein interaction motifs and link the FAK-Src complex to a number of downstream signaling pathways (10). Increased Src activity is associated with the disruption of E-cadherin–dependent AJs, and this was shown to be dependent on integrin signaling and FAK phosphorylation, indicating that the Src/FAK signaling axis may play an important role in the cross-talk between integrin- and E-cadherin–dependent adhesions (7).

Most cancer-related deaths are due to the development of metastatic disease, and several new molecularly targeted agents in clinical development (including those targeting

Authors' Affiliations: [1]Edinburgh Cancer Research Centre, Institute of Genetics and Molecular Medicine, University of Edinburgh, Edinburgh, United Kingdom and [2]Beatson Institute for Cancer Research, Glasgow, United Kingdom

Note: Supplementary data for this article are available at Cancer Research Online (http://cancerres.aacrjournals.org/).

Corresponding Author: Valerie Brunton, Edinburgh Cancer Research Centre, Edinburgh University, Crewe Road South, Edinburgh, EH4 2XR, United Kingdom. Phone: 44-131-777-3556; Fax: 44-131-777-3520; E-mail: v.brunton@ed.ac.uk.

doi: 10.1158/0008-5472.CAN-10-1454

Published OnlineFirst November 2, 2010; DOI:10.1158/0008-5472.CAN-10-1454

both Src and FAK) have the potential to prevent disease progression (11). It remains difficult, however, to assess the efficacy of antimetastatic agents in the clinical setting, and an increased understanding of how such agents work at different stages of the metastatic cascade is important in guiding their clinical use. As the tumor microenvironment plays a key role in disease progression (12) it is becoming evident that the use of appropriate animal models is essential for determining the activity of such agents. For cells to metastasize to distant sites they must undergo a number of phenotypic changes, including changes in cell-matrix and cell-cell adhesions, migration, and invasive capacity, but these have been difficult to monitor *in vivo*. Here we describe the use of optical window chambers in combination with photobleaching, photoactivation, and photoswitching to quantitatively measure collective tumor cell movement, proliferation, and protein dynamics in squamous cell carcinoma cells within a tumor mass *in vivo*. We show that inhibiting the Src/FAK signaling axis prevents the collective movement of tumor cells *in vitro* and *in vivo*, and identify a novel role for this pathway in the regulation of E-cadherin internalization, cell-cell adhesion strength, and modulation of E-cadherin dynamics downstream of β1-integrin. Taken together these data highlight the benefits of fluorescent *in vivo* imaging approaches along with the use of optical window chambers in the preclinical evaluation of potential chemotherapeutic agents, and suggest that the anti-invasive properties of small molecular inhibitors targeting Src and FAK may be mediated in part by their ability to regulate cell-cell adhesion.

Materials and Methods

Cell culture

A431 cells (LGC Promochem) were transfected with green fluorescent protein (GFP)-E-cadherin (13), pDendra2 (Evrogen), nuclear photoactivatable Green Cherry (nG^{PA}C; ref. 14), or Y527F Src-GFP (15) using the Amaxa nucleofector transfection system (Amaxa GmbH). Cells stably expressing siRNA against β1-integrin and their corresponding control cells were a kind gift from Erik Sahai (Cancer Research UK London Institute, London, UK; ref. 16). For siRNA experiments cells were transfected with 50 nmol/L of E-cadherin or FAK siRNA smartpool or siCONTROL pool1 (Dharmacon) using the Amaxa nucleofector transfection system. The following treatments were used: β1 blocking antibody, clone mAb13 (17) 2 μg/mL, 1 to 3 hours; dynasore (Sigma) 80 μmol/L, 0.5 to 2 hours; PF-562,271 (Pfizer), 250 nmol/L, 1 to 72 hours; dasatinib (Bristol-Myers Squibb) 200 nmol/L, 1 to 72 hours.

Collagen invasion assays

Cells were seeded at the bottom of transwell inserts (Corning) containing rat tail collagen type I (Roche). Transwell inserts were then placed in serum-free medium and medium supplemented with 10% FCS, and 10 ng/mL epidermal growth factor was placed on top of the gel. After 5 days, cells were stained with Calcein AM (Molecular Probes). Horizontal z-sections through the gel were taken at 10-μm intervals using an Olympus FV1000 confocal microscope. The number of positive pixels in each image was determined using Image J software (NIH). The values obtained for individual sections were normalized over the sum of values for all the sections and then expressed as a percentage of the control cell value. For each experiment, samples were run in triplicate and at least four z-series were taken per sample. Projected images used for display purposes were also created using Image J.

Dispase-based dissociation assay

Quantification of adhesion strength following mechanical stress of dispase-treated monolayers was determined as previously described (18).

Surgical implantation of optical window chambers

Optical window chambers were implanted into CD-1 nude mice under anesthesia. All animal work was carried out in compliance with UK Home Office guidelines. Optical window chambers were custom-fabricated using aluminum (19). To install the window, dorsal skin was sutured to a c-clamp template. A circle of skin was removed and screw holes were made using a 2-mm biopsy punch. The frame of the window chamber was then fitted to either side of the skin-flap and secured using screwing nuts, the tightness of which was adjusted to ensure that blood vessels were not occluded. The window was then sutured to the skin and the c-clamp was removed. A small piece of tumor was placed into the center of the window and was sealed with a coverslip. Tumors were allowed to establish under the windows for 10 days prior to imaging, at which time there was extensive revascularization (Supplementary Fig. S1A and B, Supplementary Movie S1). Further details on the optical window chambers are provided in Supplementary Methods.

Immunoblot analysis

Immunoblot analysis was performed as previously described (20). Primary antibodies used were anti-GFP (Abcam), anti-E-cadherin, anti-FAK (Becton Dickinson Transduction Laboratories), anti-pY397 FAK, anti-pY861 FAK (Biosource), anti-pY416 Src, anti-Src (Cell Signaling), β1-integrin (Chemicon), and anti-γ-tubulin (Sigma), all at 1:1,000 dilution.

Fluorescence recovery after photobleaching analysis

For *in vitro* measurements cells were maintained at 37°C in a temperature-controlled chamber, whereas animals were maintained at 37°C on a heated stage for *in vivo* measurements. Experiments were performed using an Olympus FV1000 confocal microscope with SIM scanner. For photobleaching the following settings were used: pixel dwell time 4 μs/px, pixel resolution 512 × 512, 5% (30% for *in vivo*) 488 nm laser power, pinhole 250 μm, 60× Oil 1.35 N.A. objective (40× water 0.8 N.A. for *in vivo*), and a 3× zoom. Effective photobleaching was achieved using 50% (40% for *in vivo*) 405 nm laser power, 20 μs/pixel (40 μs/pixel for *in vivo*) dwell time, and a 1 frame (3 frames for *in vivo*) bleach time. Images

Published OnlineFirst November 2, 2010; DOI:10.1158/0008-5472.CAN-10-1454

were captured every 5 seconds for 75 frames (100 frames for *in vivo*). For *in vitro* experiments, approximately 25 cells were imaged over three independent experiments, and for *in vivo* experiments five animals were imaged per condition with six movies captured from each animal. Mice were treated with PF-562,271 (33 mg/kg in 0.5% methylcellulose, p.o. by gavage) 30 minutes prior to imaging. Fluorescent intensity measurements derived from the region of interest used to bleach were averaged in Excel and used to plot recovery/decay curves. Average measurements for each time point were exported into SigmaPlot (Systat Inc) for exponential curve fitting. The half-time of recovery ($t_{1/2}$) was calculated as described previously (21).

In vivo photoswitching

Dendra2-expressing tumors were implanted in optical window chambers and imaged at 0, 6, and 24 hours after photoswitching. All images were captured using an Olympus FV1000 confocal microscope equipped with a UMPLFLN 20× 0.5 N.A. water immersion objective. Photoswitching of Dendra2 was achieved using the following settings: pixel dwell time 40 μs/px, 28% 405 nm laser power, 5 frame switching time. Mice were treated with PF-562,271 (33 mg/kg in 0.5% methylcellulose, p.o. by gavage bid) or dasatinib (15 mg/kg in 80 mmol/L citrate buffer, p.o. by gavage daily) starting on the day of photoswitching. After photoswitching a region of interest, a z-series was acquired (sections every 10 μm) for both green and red channels. Image analysis was performed using ImageJ. Each z-series was flattened into one image using the maximum z-intensity projection tool, thresholded, and the area occupied by the red fluorescent channel was measured. This area was plotted over time as a fold increase in area occupied by migrating cells.

Endocytosis of E-cadherin

Quantification of biotinylated E-cadherin endocytosis was performed as described previously (18). Further experimental details are given in Supplementary S1 Text.

Results

FAK and Src regulate A431 collective cell movement *in vitro* and *in vivo*

We had previously shown that A431 cells invade in a collective manner *in vitro*, which is dependent on the presence of E-cadherin–dependent AJs (20). Treatment of cells with either the FAK inhibitor PF-562,271 or the Src inhibitor dasatinib resulted in complete inhibition of collective cell invasion into collagen (Fig. 1A), at a concentration where FAK kinase activity (as measured by FAK autophosphorylation on Y397) and Src activity (as measured by Src autophosphorylation at Y416) were inhibited respectively (Fig. 1B). Treatment of cells with dasatinib also inhibited the Src-dependent phosphorylation of FAK on Y861 (Fig. 1B). To enable imaging and quantification of tumor cell movement *in vivo*, cells were transfected with the photoswitchable probe Dendra2 and tumors were established under observation windows (Supplementary Fig. S1A; ref. 22). A subpopulation of tumor cells was marked by switching Dendra2 from its green to red emitting state; z-sections were acquired over 24 hours (Fig. 1C), and cell movement was quantified by calculating the fold increase in area of the red fluorescence (Fig. 1D). There was extensive movement of the tumor cells over 24 hours in the vehicle-treated animals which was inhibited in both dasatinib- and PF-562,271–treated animals (Fig. 1C and D). Similar studies were carried out in cells at the edge of the tumors. Although A431 Dendra2 cells dispersed over time we rarely detected any cells moving away from the original tumor area into the surrounding stroma within the time frame of our experiments (Supplementary Fig. S2) and could therefore not use this approach to follow the invasion of the A431 cells into the surrounding stroma.

Although observation of A431 cell behavior *in vivo* indicated extensive cell movement, our results did not rule out the possible contribution of increased cell proliferation/survival to the fold increase in the area being measured. To address the contribution of proliferation and/or survival, A431 cells were transfected with a nuclear targeted photoactivatable GFP fused to mCherry ($nG^{PA}C$; ref. 14). A subpopulation of tumor cells was marked by activation of the nuclear targeted photoactivatable GFP and a confocal z-series was acquired over 24 hours (Supplementary Fig. S3A). Three-dimensional rendering and spot detection of photoactivatable GFP-marked nuclei (Supplementary Fig. S3B) was used to quantify the number of nuclei at each time point, and calculate the fold change in nuclear number (Supplementary Fig. S3C). There was a 1.2-fold increase in nuclear number over 24 hours, which was unchanged following PF-562,271 treatment. This increase in nuclear number was used to normalize measurements from Fig. 1D (Supplementary Fig. S3D). Thus, FAK kinase activity did not contribute to the proliferation/survival of A431 cells *in vivo* in the time scale of this experiment. Furthermore, the basal level of tumor cell proliferation was not sufficient to account for the fold increase in area measured following photoswitching.

E-cadherin modulates collective movement of A431 cells *in vitro* and *in vivo*

We had previously reported that loss of E-cadherin at sites of cell-cell adhesion inhibits collective invasion of A431 cells *in vitro* (20). However, overexpression of E-cadherin (2.3-fold increase; Supplementary Fig. S4A) also inhibited invasion of A431 cells into collagen (Fig. 2A), suggesting that a balance exists between E-cadherin expression and collective invasive capacity. To address whether E-cadherin overexpression affects tumor cell movement *in vivo*, cells were labeled with Dendra2 and tumors were established under observation windows. In contrast to control tumors, cells overexpressing E-cadherin exhibited a marked reduction in motility (Fig. 2B and C). Furthermore, visual observation of acquired images revealed that A431 cells maintained their collective mode of migration *in vivo* (Fig. 2D; *, individual cells within groups), suggesting that these cells are also dependent on E-cadherin–mediated cell-cell adhesions for their movement *in vivo*.

Published OnlineFirst November 2, 2010; DOI:10.1158/0008-5472.CAN-10-1454

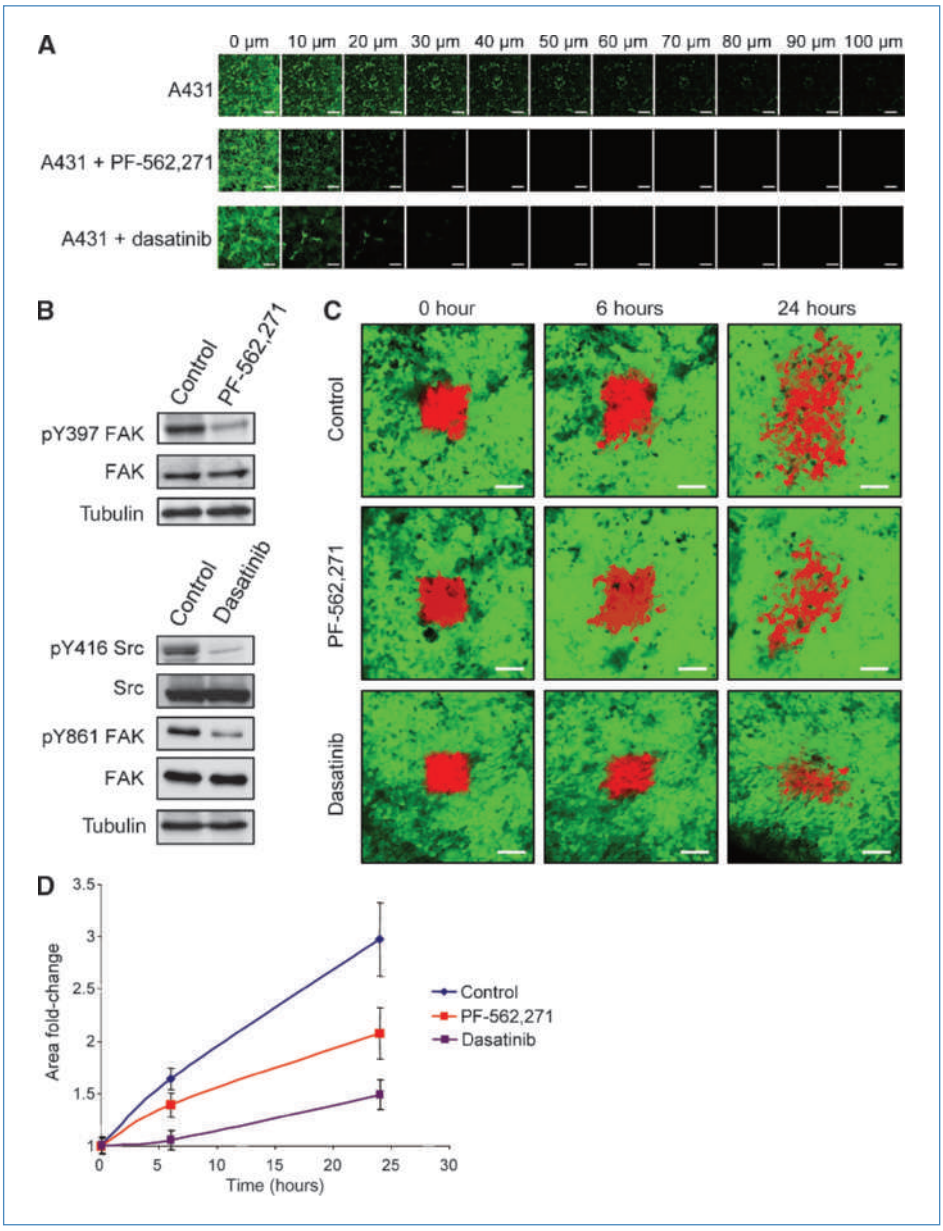

Figure 1. PF-562,271 and dasatinib inhibit collective cell movement *in vitro* and *in vivo*. A, invasion of A431 cells into collagen gels in the presence or absence of PF-562,271 or dasatinib. After 5 days, cells were labeled with calcein AM and visualized at 10-μm intervals. The experiment was performed in triplicate and representative series of z-sections at indicated depths through the gel are shown. Scale bars, 200 μm. B, immunoblot analysis of pY397 FAK and FAK expression in control and PF-562,271–treated cells, and pY416 Src, Src, pY861 FAK, and FAK in control and dasatinib-treated cells. C, images showing A431 Dendra2 control-expressing cells in tumors of untreated mice or mice treated with PF-562,271 or dasatinib, at different time points after photoswitching (red). Scale bars, 100 μm. D, quantification of the area covered by red fluorescence at shown time points. Values are the mean from at least five independent experiments. Error bars, SE.

FAK signaling regulates E-cadherin dynamics *in vitro* and *in vivo*

We have recently shown that the use of fluorescence recovery after photobleaching (FRAP) allows us to monitor E-cadherin dynamics both *in vitro* and *in vivo* (21). Changes in the recovery rate of E-cadherin molecules are associated with increased migratory potential of cells. For example, the recovery rate of GFP-E-cadherin following photobleaching in migrating cells is slower than in stationary cells, whereas inhibition of Src signaling, which reduces cell migration, increases the recovery rate of GFP-E-cadherin (21). Here we set out to determine whether changes in E-cadherin dynamics are also seen following inhibition of FAK kinase activity. GFP-E-cadherin at sites of cell-cell adhesion was subjected to photobleaching (Fig. 3A, Supplementary Movies S2 and S3). Recovery kinetics data for GFP-E-cadherin ± PF-562,271 treatment was pooled and fitted to single exponential rise-to-maximum curves (Supplementary Fig. S5A). R^2 values reflected the tight fit of our data to the predicted values (control/PF-562,271, R^2 = 0.98). Treatment of cells with PF-562,271 decreased $t_{1/2}$ by 40%. To confirm these effects were specific to inhibition of FAK kinase activity, we also used siRNA to knock down FAK expression (Supplementary Fig. S4B). A similar reduction in $t_{1/2}$ was seen in FAK knockdown cells (Fig. 3B). As FAK is an important downstream effector of

Published OnlineFirst November 2, 2010; DOI:10.1158/0008-5472.CAN-10-1454

integrin signaling we carried out FRAP of GFP-E-cadherin in cells expressing β1-integrin siRNA in which there was a specific knockdown of β1-integrin protein expression (Supplementary Fig. S4C) and also saw a reduction in $t_{1/2}$ (Fig. 3B). These results identify β1-integrin and its downstream effector FAK as key regulators of E-cadherin dynamics and show that inhibition of E-cadherin–dependent collective movement correlates with an increased rate of recovery of GFP-E-cadherin.

We next asked whether changes in E-cadherin dynamics could also be used as a readout of E-cadherin function *in vivo*. Tumors expressing GFP-E-cadherin were established under observation windows, and GFP-E-cadherin at sites of cell-cell adhesion was subjected to photobleaching (Fig. 3C, Supplementary Movies S4 and S5). Recovery kinetics data for GFP-E-cadherin in either vehicle- or PF-562,271–treated animals were pooled and fitted to single exponential rise-to-maximum curves (Supplementary Fig. S5B). R^2 values reflected the tight fit of our

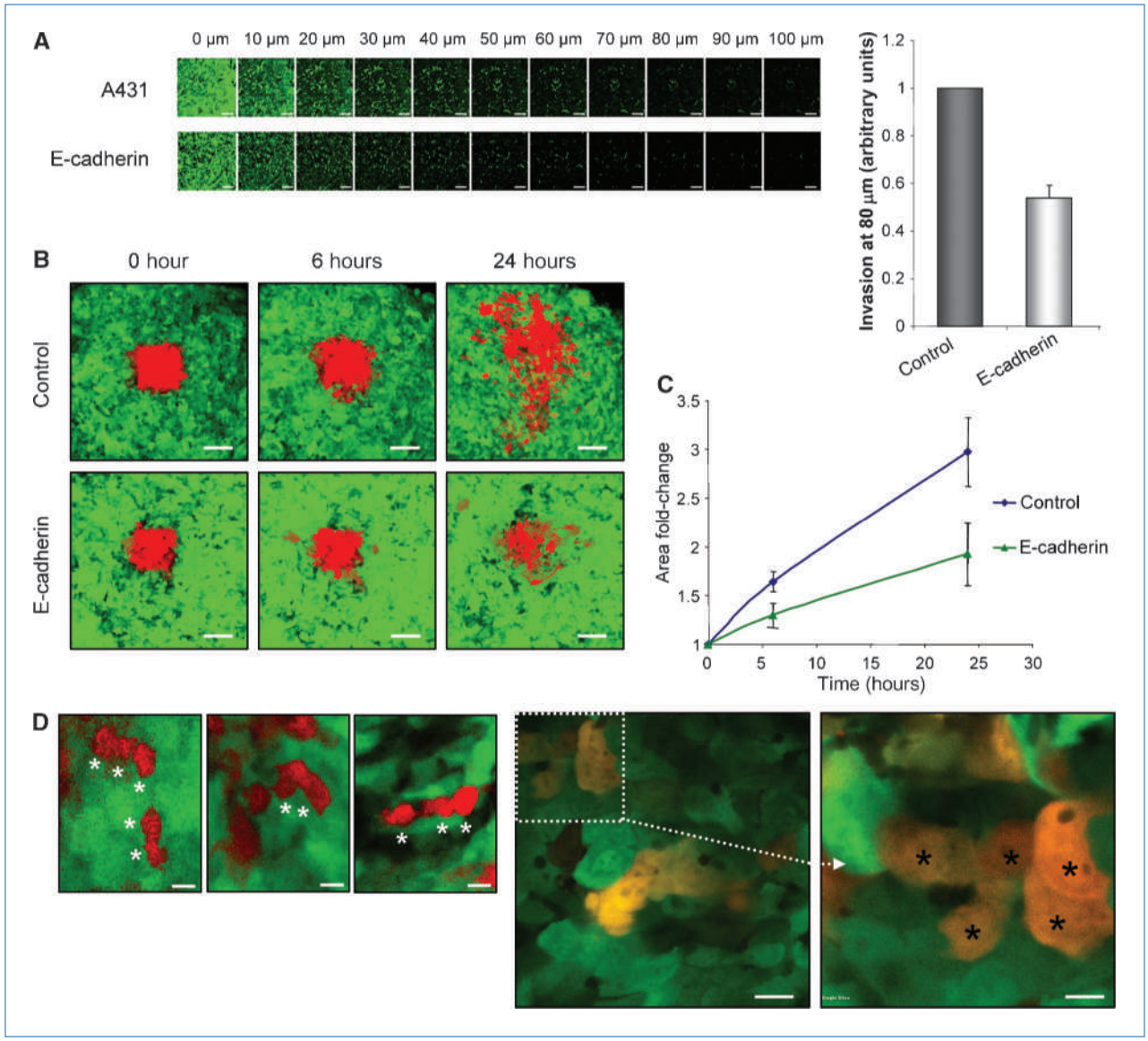

Figure 2. E-cadherin modulates collective cell movement *in vitro* and *in vivo*. A, invasion of A431 and A431 GFP-E-cadherin cells into collagen gels. After 5 days, cells were labeled with calcein AM and visualized at 10-μm intervals. Representative series of z-sections at indicated depths through the gel are shown. Scale bars, 200 μm. Quantification of invasion at 80 μm is shown for a representative experiment in a series of three. Values are the mean from triplicate wells. B, images showing A431 Dendra2 control or GFP-E-cadherin–expressing cells in tumors at different time points after photoswitching (red). Scale bars, 100 μm. C, quantification of the area covered by red fluorescence at shown time points. Values are the mean from at least five independent experiments. A and C, error bars, SE. D, zoomed images from B (left) and higher magnification images (center and right) showing collective cell movement. *, individual cells within a group; scale bars, 20 μm (left and center images) and 10 μm (right image).

Published OnlineFirst November 2, 2010; DOI:10.1158/0008-5472.CAN-10-1454

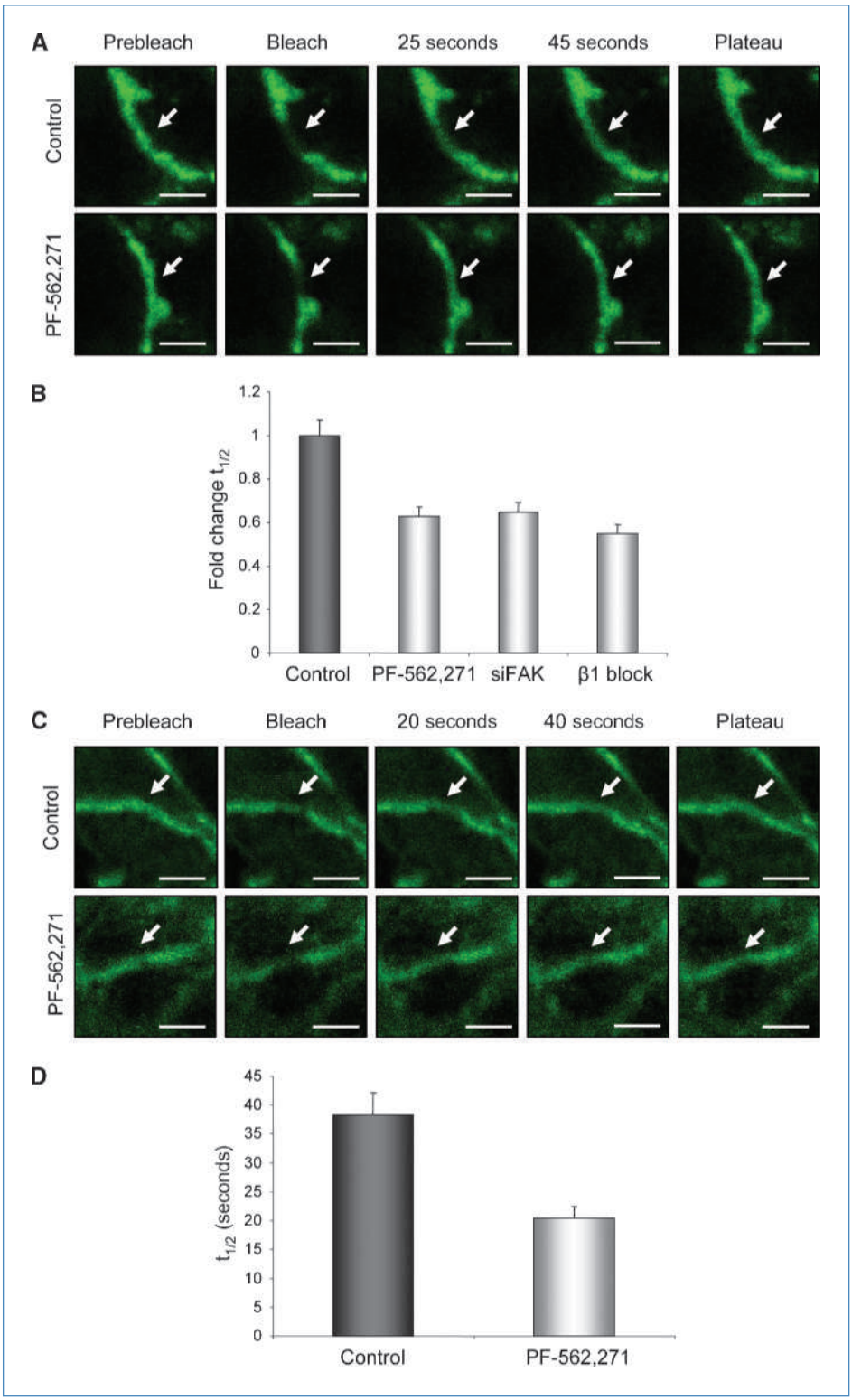

Figure 3. PF-562,271 alters E-cadherin dynamics *in vitro* and *in vivo*. A, still images of GFP-E-cadherin at cell-cell junctions in untreated cells (top) or cells treated with PF-562,271 (bottom) captured prebleach and following bleach. Scale bar, 5 μm. Arrows, bleached area (B) $t_{1/2}$ of GFP-E-cadherin in control cells or cells treated with PF-562,271, FAK siRNA, or β1-integrin blocking antibody. C, still images of GFP-E-cadherin at cell-cell junctions in tumors untreated (top) or treated with PF-562,271 (bottom) captured prebleach and following bleach. Arrows, bleached areas (D) $t_{1/2}$ of GFP-E-cadherin in tumors from control or PF-562,271 treated mice. A and C, scale bars, 5 μm. B and D, values are the mean from at least 25 cells. Error bars, SE.

data to the predicted values (control/PF-562,271, $R^2 = 0.97$). Treatment of animals with PF-562,271 prior to photobleaching of GFP-E-cadherin resulted in a marked reduction in $t_{1/2}$ (control, 38.3 ± 3.2 seconds; PF-562,271, 20.4 ± 2.5 seconds; Fig. 3D), similar to that observed *in vitro*. Thus, inhibition of FAK kinase activity following treatment with PF-562,271 results in altered E-cadherin dynamics *in vivo*, which correlates with reduced E-cadherin–dependent collective cell movement.

Published OnlineFirst November 2, 2010; DOI:10.1158/0008-5472.CAN-10-1454

FAK controls E-cadherin internalization and cell-cell adhesion strength downstream of β1-integrin

The observation that E-cadherin overexpression and inhibition of Src/FAK signaling both resulted in inhibition of invasion and the ability of Src/FAK to regulate E-cadherin dynamics both *in vitro* and *in vivo* led us to hypothesize that inhibiting the Src/FAK signaling axis may regulate the collective movement of A431 cells via regulation of E-cadherin. It has been previously reported that the level of E-cadherin protein at sites of cell-cell adhesion regulates cadherin adhesiveness (23). Thus, we hypothesized that increased E-cadherin expression at these sites may inhibit cell movement by increasing cell-cell adhesion strength. To determine the effect of E-cadherin expression on cell-cell adhesion strength we treated confluent cultures with dispase, which results in detachment of the cells in an intact monolayer. The resistance to disaggregation induced by mechanical stress of these monolayers was then used as a measure of the relative strength of cell-cell contacts. Overexpression of E-cadherin resulted in a reduction in the number of single cells detached from the cell sheets, whereas inhibition of E-cadherin expression by siRNA decreased adhesion strength (Fig. 4A), indicating a crucial role for E-cadherin in A431 cell-cell adhesion strength. Treatment of cells with PF-562,271 or knockdown of FAK by siRNA was also observed to increase cell-cell adhesion strength (Fig. 4A). Furthermore, inhibition of Src kinase activity by dasatinib increased cell-cell adhesion strength (Fig. 4A). However, this was not mediated by increased expression of E-cadherin in the inhibitor-treated cells (Supplementary Fig. S6).

To explore the signaling events taking place upon β1-integrin inhibition, we looked at activation of both FAK

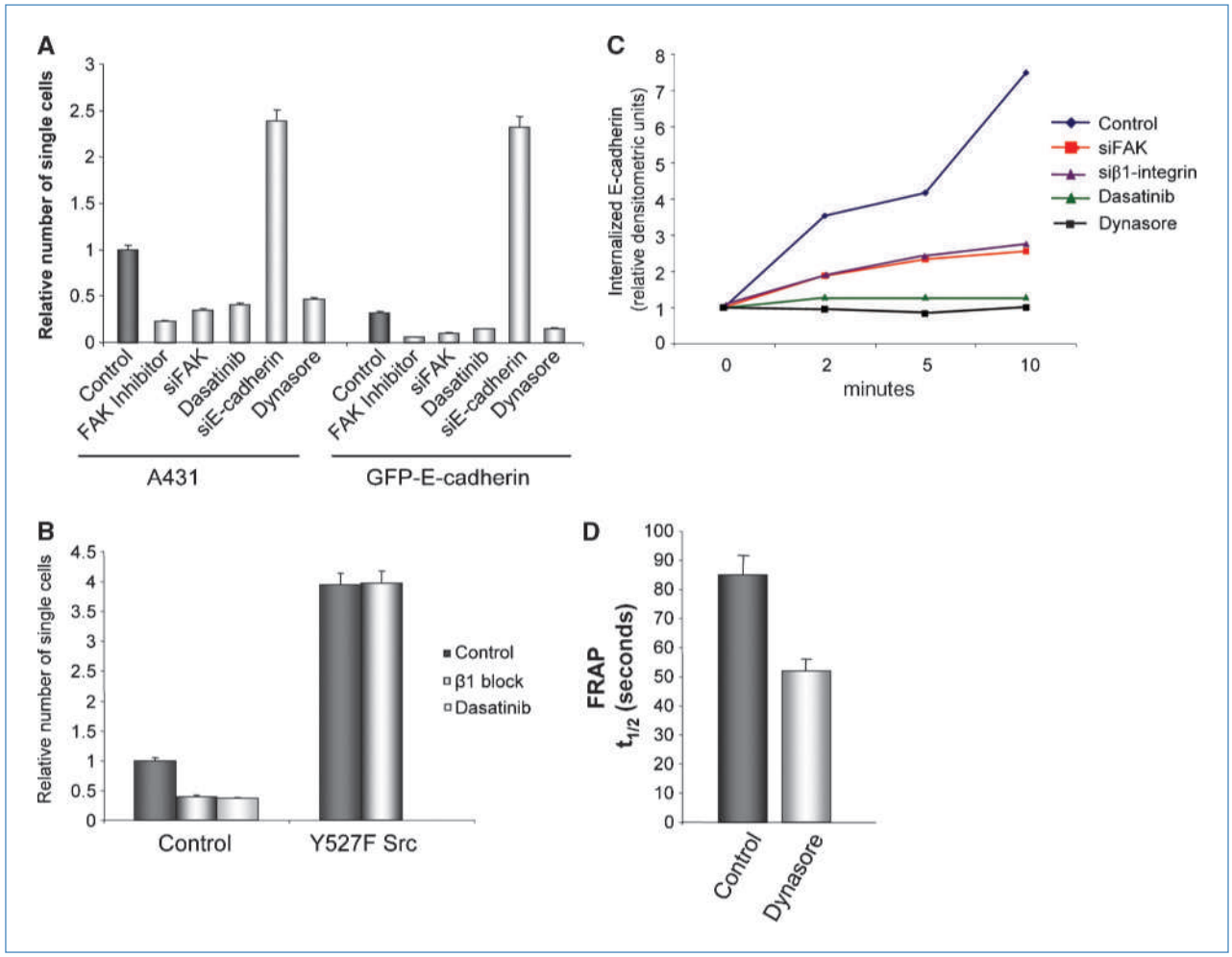

Figure 4. Inhibition of Src-dependent phosphorylation of FAK downstream of β1-integrin disrupts E-cadherin endocytosis and strengthens cell-cell junctions. A, number of single cells that disaggregate from a dispase-treated monolayer. Values represent the mean from at least three independent experiments. B, number of single cells that disaggregate from a dispase-treated monolayer in control and Y527F Src-expressing cells in the presence or absence of β1-integrin blocking antibody or dasatinib. Values represent the mean from at least three independent experiments. C, quantification of biotinylated E-cadherin internalization over 10 minutes in control or FAK siRNA cells, β1-integrin siRNA cells, control cells treated with dasatinib or dynasore. D, $t_{1/2}$ of GFP-E-cadherin in control or dynasore-treated cells. Values are the mean from at least 25 cells. A, B, and D, error bars, SE.

Published OnlineFirst November 2, 2010; DOI:10.1158/0008-5472.CAN-10-1454

and Src in β1-integrin siRNA–expressing cells. With vinculin used as a marker of integrin adhesions, activation of both Src and FAK in control cells was detected in integrin adhesions (Supplementary Fig. S4D). In cells lacking β1-integrin, however, although FAK was active at integrin adhesions (as measured by pY397 FAK), active Src was absent and there was no detectable pY861 FAK (Supplementary Fig. S4D). Thus, cells lacking β1-integrin are still able to assemble cell-matrix adhesions that contain active FAK. This may be due to incomplete knockdown of β1-integrin in the cells or signaling to Y397 FAK from other β-integrin subunits (16). However, active Src was absent from these adhesions and therefore unable to phosphorylate FAK. Disruption of β1-integrin signaling therefore specifically prevents activation of Src at integrin adhesion sites. In contrast, active Src was still present at integrin adhesion sites in FAK knockdown cells (Supplementary Fig. S4E), whereas the amount of activated Src bound to FAK in wild-type cells was decreased in the presence of PF-562,271, as detected by immunoprecipitation (Supplementary Fig. S4F). Thus, molecular characterization of signaling through Src and FAK in both FAK and β1-integrin knockdown cells highlighted a single common event: suppression of Src-dependent phosphorylation of FAK at integrin adhesions, either mediated via loss of activated Src from integrin adhesions (as seen in β1-integrin knockdown cells) or its inability to bind to FAK either through loss of FAK protein (as seen in FAK knockdown cells) or kinase inhibition (PF-562,271–treated cells). Taken together with the ability of dasatinib to prevent phosphorylation of FAK on Y861, this suggests that the observed effects on E-cadherin and adhesion strength may be mediated via the Src-dependent phosphorylation of FAK.

To confirm that the ability of Src and FAK to regulate E-cadherin–dependent AJs required the Src-dependent phosphorylation of FAK downstream of β1-integrin signaling we expressed a constitutively active Src mutant (Y527F Src) in A431 cells. Western blotting showed that activated Src and pY861 FAK were increased in cells expressing Y527F Src (Supplementary Fig. S4G). Constitutive activation of Src resulted in a weakening of cell-cell adhesions as measured by an increase in single cells following mechanical disruption (Fig. 4B) without causing complete dissolution of cell-cell junctions (Supplementary Fig. S4H). Treatment with a β1-integrin blocking antibody decreased the number of single cells in control cultures but had no effect in cells expressing activated Src (Fig. 4B). Thus, strengthening of cell-cell junctions following inhibition of β1-integrin is prevented when Src is constitutively active, indicating that expression of an unregulated active Src negates the ability of β1-integrin to control adhesion strength. Furthermore, treatment of cells with dasatinib prevented phosphorylation of FAK on Y861 and increased adhesion strength (Figs. 1B and 4A), indicating that Src-dependent phosphorylation of FAK downstream of β1-integrin regulates adhesion strength.

As treatment with PF-562,271 or dasatinib did not alter total E-cadherin protein levels (Supplementary Fig. S6), Src/FAK signaling must regulate E-cadherin function by other mechanisms. E-cadherin–mediated cell-cell junctions are highly dynamic structures and the concentration of E-cadherin specifically at cell-cell junctions is controlled by endocytosis, which in turn regulates adhesion strength. To measure endocytosis we followed the internalization of biotinylated cell surface E-cadherin: biotinylated cell surface E-cadherin was progressively enriched in the intracellular pool in control cells whereas in cells treated with dynasore, a potent dynamin inhibitor that blocks vesicles pinching off the membrane (24), there was no internalization of E-cadherin (Fig. 4C). E-cadherin internalization was reduced in β1-integrin siRNA cells (Fig. 4C). A similar reduction in E-cadherin internalization was seen in cells treated with dasatinib or when FAK expression was knocked down (Fig. 4C).

In support of a link between E-cadherin internalization and adhesion strength, treatment of cells with dynasore also increased adhesion strength (Fig. 4A). Furthermore, FRAP analysis of dynasore-treated cells showed a reduction in the $t_{1/2}$ of GFP-E-cadherin, as was seen following inhibition of Src/FAK signaling (Fig. 4D). Thus, although measurement of E-cadherin–mediated cell-cell adhesion strength and E-cadherin internalization is not possible *in vivo*, changes in the $t_{1/2}$ may represent an indirect readout of E-cadherin function that can be measured *in vivo*.

Discussion

We have identified a novel role for Src and FAK in regulating E-cadherin function that is required for the collective movement of tumor cells. In human tumors loss of E-cadherin is associated with more aggressive and invasive tumors. It is now evident, however, that the collective movement of tumors, which is dependent on the maintenance of cell-cell junctions, also plays a key role in the invasive capacity of tumors (6). A tight balance exists between E-cadherin expression and collective movement, and the dynamic regulation of E-cadherin at cell-cell junctions is crucial in determining junction strength, which we had previously linked to the migratory capacity of tumor cells *in vitro* (21). Here we show that Src/FAK signaling downstream of β1-integrin controls E-cadherin internalization and adhesion strength *in vitro*. Functional measurements of E-cadherin–mediated cell-cell adhesion strength and E-cadherin internalization are not currently possible *in vivo*, and it is therefore important to utilize techniques such as FRAP to monitor E-cadherin dynamics that can provide an indirect readout of E-cadherin function that would otherwise not be possible *in vivo*. The ability of small molecule inhibitors of Src and FAK to alter E-cadherin dynamics *in vivo* correlated with their ability to strengthen cell-cell adhesion, inhibit E-cadherin internalization, and importantly inhibit the collective movement of A431 cells *in vivo*. Src and FAK can regulate cell invasion *in vitro* through their role in regulating cell migration and matrix metalloproteinase activity at sites of invadopodia (25–29). These findings identify a novel additional mechanism through which β1-integrin signaling via Src-dependent phosphorylation of FAK may regulate the collective movement of tumor cells by modulating

Published OnlineFirst November 2, 2010; DOI:10.1158/0008-5472.CAN-10-1454

cell-cell adhesion strength through control of E-cadherin internalization.

Previously skin flaps were used to monitor the movement of tumor cells *in vivo*, but studies using this method are restricted by the short period of time that migration can be monitored and the infrequency that individual cells move *in vivo* within these time frames. To overcome these problems we utilized optical window chambers, which together with recoverable anesthesia, enabled the repeated imaging of animals over several days. In addition, in contrast to skin flaps, observation windows do not require invasive surgery immediately prior to imaging, and therefore preserve the local tumor microenvironment by minimizing the risk of inflammatory response and tissue damage as a consequence of surgery. Furthermore, images acquired using this method displayed improved signal to noise and increased sample stability, when compared with our previously reported use of skin flaps for FRAP (21). A comparison of FRAP data acquired *in vivo* using skin flaps and optical window imaging methods is shown in Supplementary Fig. S5C and D. The resulting FRAP dataset obtained through the observation windows exhibited R^2 values comparable with those only previously possible *in vitro*. To enable the imaging and quantification of tumor cell movement *in vivo* we combined the implantation of observation windows with the specific labeling of tumor cells using the photoswitchable protein Dendra2, in a similar manner to that recently reported by Kedrin and colleagues (22). Photoswitching of Dendra2 from its green to red emitting state permitted long-term monitoring of tumor cell behavior. In addition, use of the nuclear targeted photoactivatable probe $G^{PA}C$ (14) enabled the quantification of nuclear division *in vivo*. Thus, photoswitchable and photoactivatable probes, together with recoverable imaging using optical window chambers, can be used to implement robust and reproducible assays for monitoring the movement and proliferation of tumor cells *in vivo* and provide invaluable information regarding drug action that can help to dissect out the mechanism of action of new therapeutics.

Disclosure of Potential Conflicts of Interest

No potential conflicts of interest were disclosed.

Grant Support

Cancer Research UK Program Grant C157/A9148.

The costs of publication of this article were defrayed in part by the payment of page charges. This article must therefore be hereby marked *advertisement* in accordance with 18 U.S.C. Section 1734 solely to indicate this fact.

Received 04/23/2010; revised 08/18/2010; accepted 09/15/2010; published OnlineFirst 11/02/2010.

References

1. Thiery JP. Cell adhesion in development: a complex signaling network. Curr Opin Genet Dev 2003;13:365–71.
2. Nelson WJ. Adaptation of core mechanisms to generate cell polarity. Nature 2003;422:766–74.
3. Hajra KM, Fearon ER. Cadherin and catenin alterations in human cancer. Genes Chromosomes Cancer 2002;34:255–68.
4. Nollet F, Berx G, van Roy F. The role of the E-cadherin/catenin adhesion complex in the development and progression of cancer. Mol Cell Biol Res Commun 1999;2:77–85.
5. Yap AS. The morphogenetic role of cadherin cell adhesion molecules in human cancer: a thematic review. Cancer Invest 1998;16:252–61.
6. Friedl P, Gilmour D. Collective cell migration in morphogenesis, regeneration and cancer. Nat Rev Mol Cell Biol 2009;10:445–57.
7. Avizienyte E, Wyke AW, Jones RJ, et al. Src-induced de-regulation of E-cadherin in colon cancer cells requires integrin signalling. Nat Cell Biol 2002;4:632–8.
8. Playford MP, Vadali K, Cai X, Burridge K, Schaller MD. Focal adhesion kinase regulates cell-cell contact formation in epithelial cells via modulation of Rho. Exp Cell Res 2008;314:3187–97.
9. Chen X, Gumbiner BM. Crosstalk between different adhesion molecules. Curr Opin Cell Biol 2006;18:572–8.
10. Schlaepfer DD, Mitra SK, Ilic D. Control of motile and invasive cell phenotypes by focal adhesion kinase. Biochim Biophys Acta 2004;1692:77–102.
11. Brunton VG, Frame MC. Src and focal adhesion kinase as therapeutic targets in cancer. Curr Opin Pharmacol 2008;8:427–32.
12. Joyce JA, Pollard JW. Microenvironmental regulation of metastasis. Nat Rev Cancer 2009;9:239–52.
13. Miranda KC, Khromykh T, Christy P, et al. A dileucine motif targets E-cadherin to the basolateral cell surface in Madin-Darby canine kidney and LLC-PK1 epithelial cells. J Biol Chem 2001;276:22565–72.
14. Welman A, Serrels A, Brunton VG, Ditzel M, Frame MC. A two color photoactivatable probe for selective tracking of proteins and cells. J Biol Chem 2010;285:11607–16.
15. Sandilands E, Cans C, Fincham VJ, et al. RhoB and actin polymerization coordinate Src activation with endosome-mediated delivery to the membrane. Dev Cell 2004;7:855–69.
16. Brockbank EC, Bridges J, Marshall CJ, Sahai E. Integrin β1 is required for the invasive behaviour but not proliferation of squamous cell carcinoma cells *in vivo*. Br J Cancer 2005;92:102–12.
17. Akiyama SK, Yamada SS, Chen WT, Yamada KM. Analysis of fibronectin receptor function with monoclonal antibodies: roles in cell adhesion, migration, matrix assembly, and cytoskeletal organization. J Cell Biol 1989;109:863–75.
18. Canel M, Serrels A, Anderson KI, Frame MC, Brunton VG. Use of photoactivation and photobleaching to monitor the dynamic regulation of E-cadherin at the plasma membrane. Cell Adh Migr 2010;4:489–99.
19. Makale M. Intravital imaging and cell invasion. Methods Enzymol 2007;426:375–401.
20. Macpherson IR, Hooper S, Serrels A, et al. p120-catenin is required for the collective invasion of squamous cell carcinoma cells via a phosphorylation-independent mechanism. Oncogene 2007;26:5214–28.
21. Serrels A, Timpson P, Canel M, et al. Real-time study of E-cadherin and membrane dynamics in living animals: implications for disease modeling and drug development. Cancer Res 2009;69:2714–9.
22. Kedrin D, Gligorijevic B, Wyckoff J, et al. Intravital imaging of metastatic behavior through a mammary imaging window. Nat Methods 2008;5:1019–21.

Published OnlineFirst November 2, 2010; DOI:10.1158/0008-5472.CAN-10-1454

23. Yap AS, Brieher WM, Pruschy M, Gumbiner BM. Lateral clustering of the adhesive ectodomain: a fundamental determinant of cadherin function. Curr Biol 1997;7:308–15.
24. Macia E, Ehrlich M, Massol R, Boucrot E, Brunner C, Kirchhausen T. Dynasore, a cell-permeable inhibitor of dynamin. Dev Cell 2006;10: 839–50.
25. Zhang Y, Thant AA, Hiraiwa Y, et al. A role for focal adhesion kinase in hyluronan-dependent MMP-2 secretion in a human small-cell lung carcinoma cell line, QG90. Biochem Biophys Res Commun 2002; 290:1123–7.
26. Hsia DA, Mitra SK, Hauck CR, et al. Differential regulation of cell motility and invasion by FAK. J Cell Biol 2003;160:753–67.
27. Hauck CR, Hsia DA, Puente XS, Cheresh DA, Schlaepfer DD. FRNK blocks v-Src-stimulated invasion and experimental metastases without effects on cell motility or growth. EMBO J 2002;21: 6289–302.
28. Hauck CR, Hsia DA, Ilic D, Schlaepfer DD. v-Src SH3-enhanced interaction with focal adhesion kinase at β 1 integrin-containing invadopodia promotes cell invasion. J Biol Chem 2002;277: 12487–90.
29. Canel M, Secades P, Garzon-Arango M, et al. Involvement of focal adhesion kinase in cellular invasion of head and neck squamous cell carcinomas via regulation of MMP-2 expression. Br J Cancer 2008; 98:1274–84.